

## Electronic transport through bent carbon nanotubes: Nanoelectromechanical sensors and switches

Amir A. Farajian,<sup>1,\*</sup> Boris I. Yakobson,<sup>2</sup> Hiroshi Mizuseki,<sup>1</sup> and Yoshiyuki Kawazoe<sup>1</sup>

<sup>1</sup>*Institute for Materials Research, Tohoku University, Sendai 980-8577, Japan*

<sup>2</sup>*Center for Nanoscale Science and Technology, Department of Mechanical Engineering and Materials Science, Rice University, Houston, Texas 77251-1892*

(Received 16 December 2002; published 30 May 2003)

We theoretically investigate the mechanical deformations of armchair, zigzag, and zigzag-armchair kink nanotube structures, under severe bendings, within a tight-binding model. It is shown that the zigzag tube is stiffer than the armchair tube with the same diameter. The kink structure is found to be quite stable under severe bendings. Calculating the  $I$ - $V$  characteristics, we show that, at the same bias, the current of metallic tube decreases with increased bending, while that of semiconducting tube increases. Such a universal behavior is not observed for the kink structure due to two competing effects. Possible application to nanoelectromechanical sensors and switches is discussed.

DOI: 10.1103/PhysRevB.67.205423

PACS number(s): 62.25.+g, 72.80.Rj, 73.63.Fg

### I. INTRODUCTION

The mechanical properties of carbon nanotubes, together with their electronic properties, provide a unique and promising basis for theoretical investigations, as well as practical applications. Previous calculations of the nanotubes Young modulus, using empirical force-constant<sup>1</sup> and *ab initio*<sup>2</sup> models, indicate that it is independent of the chirality of the tube. However, for larger strains, it is shown<sup>3</sup> that most of the axial strain is borne by the bonds parallel to the tube axis. Therefore, one may naturally expect a difference between the mechanical response of the tubes possessing bonds parallel to the tube's axis—i.e., zigzag tubes—and that of the tubes without such bonds (e.g., armchair tubes). It is indeed shown,<sup>4</sup> using a tight-binding model, that the mechanical response of the nanotubes under large strain is helicity dependent.

As concerns the bending phenomena in carbon nanotubes, several experiments<sup>5–8</sup> have indicated that, under severe bendings, buckling is the usual way for the nanotubes to reduce strain. The usual approach to the theoretical modeling of buckling phenomena has so far made use of classical potentials.<sup>6,9,10</sup> Even for calculations of the electronic properties of the bent tubes, which make use of relatively more sophisticated quantum tight-binding Hamiltonians, the starting geometry of the bent nanotubes has been obtained using classical potentials.<sup>11–13</sup> The relaxation procedure based on classical potentials does not take into account the increased  $\sigma$ - $\pi$  hybridization as a result of bending, especially at larger bending angles. However, the increased hybridization is expected to have a decisive effect not only on electronic structure, but also on the forces and relaxed atomic configurations themselves.

The interrelationship of the electronic and mechanical properties of carbon nanotubes<sup>11–17</sup> gives rise to natural speculations for possible applications. It has been shown both experimentally<sup>18</sup> and theoretically<sup>19,20</sup> that the reversible bending of nanotubes can be used to alter their conduction, which, in turn, may be used in nanoelectromechanical

switch and sensor applications.

Here, we investigate electronic transport through bent carbon nanotubes and establish a correspondence between the mechanical deformation and current that is passing across the deformed region. First, we obtain the optimized configurations of the bent armchair, zigzag, and zigzag-armchair kink<sup>21–23</sup> structures, using a four-orbital-per-atom tight-binding model. Next, the conductance characteristics of the relaxed structures are derived. Finally, we calculate the current passing through the bent nanotubes and focus on the effects of bending angle on the current-voltage ( $I$ - $V$ ) features.

### II. MODEL AND METHOD

In order to obtain relaxed structures under bending and to calculate transport properties, three different nanotubes are considered in this study: a (6,6) armchair, a (10,0) zigzag, and a (10,0)-(6,6) zigzag-armchair kink structure, which contain 972, 940, and 974 carbon atoms, respectively. [The diameters of the (6,6) armchair and (10,0) zigzag nanotubes are 8.1 and 7.8 Å, respectively.] The lengths of these portions are 98 Å for the armchair and zigzag tubes and 100 Å for the kink configuration. Considering the large number of atoms in the systems that makes *ab initio* geometry optimization formidable and taking into account the disadvantage of using classical potentials mentioned above, we choose a four-orbital-per-atom tight-binding approach, with the parametrization for carbon of Xu *et al.*,<sup>24</sup> both to obtain the optimized geometries and to calculate the electronic and transport properties. This parametrization has proved to provide a transferable potential in tight-binding studies of carbon systems and has recently been applied to the study of C<sub>60</sub>-doped nanotubes<sup>25</sup> and nanotubes under large strain.<sup>4</sup> Geometry optimizations are performed via the O(N) density-matrix electronic structure calculation method of Li *et al.*,<sup>26</sup> combined with the Broyden minimization scheme,<sup>27</sup> within the above-mentioned tight-binding approach.<sup>28</sup>

The optimization of the bent structures proceeds as follows. For successive bending angles, while fixing eight car-

bon rings (96 atoms for the armchair case and 80 atoms for the zigzag case) at each end of the nanotube, the structure is optimized such that the maximum force acting on the unconstrained atoms becomes less than  $0.05 \text{ eV/\AA}$ .

Having obtained the relaxed structures for different bending angles, we focus on the transport properties. In calculating the conductance,  $G(E, V) = (2e^2/h)T(E, V)$ , two semi-infinite perfect nanotubes—i.e., “leads,”—are assumed to be attached to the two ends of the bent region. Here, the transmission  $T(E, V)$  across the bent region is a function of energy  $E$  and bias voltage  $V$  applied to the bent region.  $T(E, V)$  is determined by calculating the total Green’s function of the system projected onto the bent region,<sup>29–34</sup> as applied previously to the calculations of transport through various nanotube heterostructures.<sup>35,12,13</sup> The  $I$ - $V$  characteristics are then obtained using the Landauer-Büttiker formula<sup>36</sup>

$$I(V) = \frac{2e}{h} \int dE T(E, V) [f_B(E - \mu_B) - f_A(E - \mu_A)], \quad (1)$$

where  $f_A$  and  $f_B$  are the Fermi distributions of the two semi-infinite perfect tubes connected to the bent region. When a bias voltage  $V$  is applied to the bent region, the chemical potentials of the two leads,  $\mu_A$  and  $\mu_B$ , are assumed to be pinned at  $V/2$  and  $-V/2$ . This determines the shifts of the band structures and density of states (DOS) of the leads. This is achieved by shifting the on-site elements of the tight-binding Hamiltonians of the two leads by  $V/2$  and  $-V/2$ . Within the bent region, on the other hand, the on-site shifts are determined by the potential drop pattern. As for the functional form of the potential drop, which is necessary in calculating  $I$ - $V$  characteristics, we assume a linear drop across the bent region. Although a self-consistent calculation of the accurate pattern of the potential drop<sup>35,37</sup> is possible in principle, applying this approach to the bent nanotubes of this study is currently formidable, due to the large number of carbon atoms involved. Our assumption of linear drop is justified by the observation that, as we shall see shortly, the deformations within the bent nanotubes are distributed more or less uniformly.

### III. RESULTS AND DISCUSSION

#### A. Mechanical response

The results of geometry optimizations are depicted in Fig. 1 for armchair and zigzag structures and in Fig. 2 for the zigzag-armchair kink structure. Comparing the results shown in Fig. 1 with the previous optimized structures obtained using classical potentials for the armchair<sup>11,12</sup> and zigzag<sup>6</sup> configurations, we notice an overall extension of the bent region in the tight-binding results as compared to the classical results. This is attributed to including the increased  $\sigma$ - $\pi$  hybridization within the tight-binding model, especially at larger bending angles. It is true that the sharp bucklings observed in the results of classical relaxations are in apparent consistency with the experimental results of Iijima *et al.*<sup>6</sup> for bent single-wall nanotubes. However, one cannot rule out the possibility of the presence of mechanical defects at the buckling position in experimental results, which can result in the

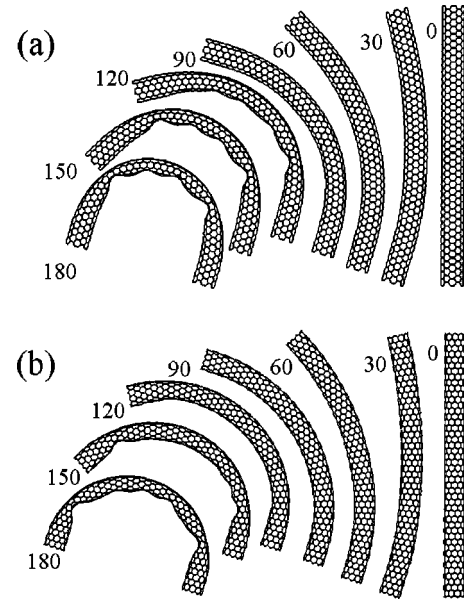


FIG. 1. Relaxed configurations of the (6,6) armchair (a) and (10,0) zigzag (b) tubes at different bending angles.

sharp buckling. The effects of surrounding environment should not be discarded in interpreting the experimental results either, especially for the bent multiwall tubes reported by Despres *et al.*<sup>5</sup> and Iijima *et al.*<sup>6</sup> It should be mentioned that smooth bending of multiwall nanotubes is also observed experimentally,<sup>5,7</sup> where the effects of the surroundings are less interfering.

Another interesting feature of Fig. 1 is the clear difference between the mechanical response of armchair and zigzag tubes: Although for small bending angles the optimized structures show no sign of buckling in both armchair and zigzag cases, for bending angles equal and bigger than  $120^\circ$ ,

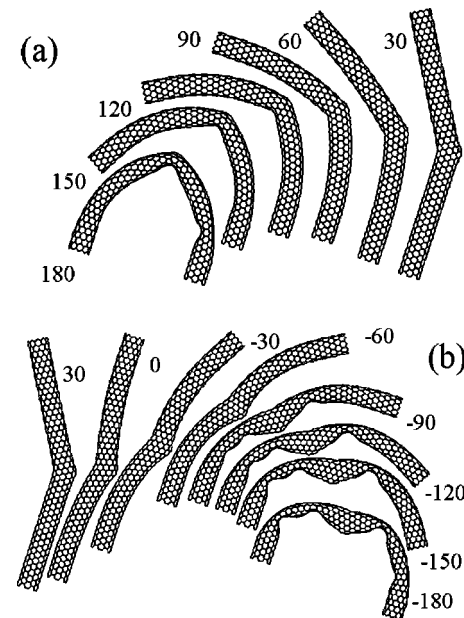


FIG. 2. Relaxed configurations of the (10,0)-(6,6) kink structure under different positive (a) and negative (b) bending angles.

the zigzag structure appears to be stiffer. This is further manifested in Fig. 2, where, under successively larger bendings, the armchair part of the structure buckles earlier and appears to be more ductile. The reason for this asymmetry is that in the zigzag structure there are bonds parallel to the tube's axis, while such bonds do not exist in the armchair structure. In accordance with a previous tight-binding study<sup>3</sup> of nanotubes under uniaxial compression, our results show that the significant bonds, responsible for bearing most of the axial strain, are indeed bonds parallel to the tube axis.

Figure 2 further shows that the zigzag-armchair kink structure, despite including a pentagon-heptagon defect, is quite stable under severe bendings: Bending the kink structure either "positively" or "negatively" (see Fig. 2) does not result in bond breaking or the formation of plastic defects, such as plastic flow and/or extra pentagon-heptagon cores<sup>38</sup> or a collapse from graphite ( $sp^2$ ) to diamond ( $sp^3$ ) structure.<sup>3,18,19</sup>

Same results of defect-free  $sp^2$  relaxed structures are seen to hold for pure armchair and zigzag tubes in Fig. 1: A quantitative analysis of the bond lengths in the relaxed structures of Figs. 1 and 2, along the line performed by Maiti *et al.*,<sup>20</sup> reveals that for the severely deformed structures of armchair (6,6)@180°, zigzag (10,0)@180°, kink (10,0)-(6,6)@180°, and kink (10,0)-(6,6)@-180° the C-C bond lengths between each carbon atom and its three nearest neighbors lie within 1.35 and 1.60 Å. The fourth nearest neighbor, however, does not appear until the C-C bond length is increased to 2.15 for (10,0)@180°, 2.20 for (10,0)-(6,6)@180°, and 2.25 Å for (6,6)@180°/(10,0)-(6,6)@-180°, respectively. This indicates that there is no change in the number of nearest neighbors even up to the maximum bending angle considered here, i.e., 180°.

## B. Conductance

The conductance characteristics of the relaxed bent structures, at zero bias, are calculated at different carrier energies, assuming two semi-infinite perfect tubes to be attached to the two ends of the bent region. In Fig. 3, we show the conductance results for the armchair (6,6) and zigzag (10,0), at different bending angles. Figure 4 illustrates the conductance characteristics of the bent kink (10,0)-(6,6) structures. It is evidently seen from Fig. 3 that there is no indication of a metal-to-semiconductor or semiconductor-to-metal transition. In other words, the conductance of the metallic armchair tube at Fermi energy remains nonzero, even under severe bendings. And there is no conducting state produced within the gap of the bent semiconducting zigzag tube. For the case of a semiconducting zigzag tube, this result could be expected, based on the fact that no matter how the finite bent region is mechanically modified, the semi-infinite nanotube leads, being semiconducting zigzag (10,0) themselves, do not possess any conducting channel within their gaps. That is, irrespective of how charge carriers are scattered within the bent region, they cannot find a way out through the semi-infinite leads, at energies within the gap. The same reason applies to the conductance of the bent kink structures, where the gap persists upon bending, due to the lack of conducting

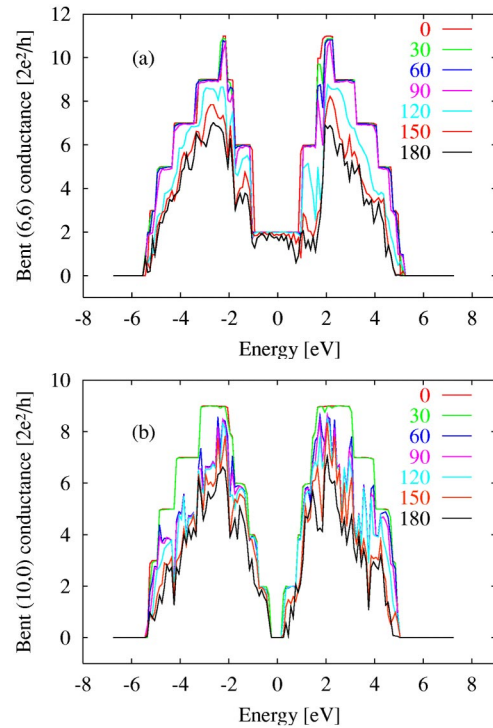


FIG. 3. (Color online) Conductance characteristics of bent (6,6) (a) and (10,0) (b) nanotubes at different bending angles. The Fermi energy is shifted to zero.

channels within the semi-infinite zigzag lead attached to the zigzag part of the bent region.

From Figs. 3 and 4, the conductance of armchair, zigzag, and kink structures is observed to reduce rather smoothly upon bending, with an average maximum reduction of less than 50% for the largest bending angles. Interestingly, despite the severely deformed portions observed at large bending angles, we do not observe the dramatic decrease of conductance by several orders of magnitude observed in the experiments of slightly bent tubes by atomic force microscope<sup>18</sup> (AFM) and their corresponding relaxed  $sp^2$  theoretical results.<sup>20</sup> This difference is attributed to the fact that in both the experimental and theoretical investigations, the presence of the AFM tip causes a severe deformation which is uniquely localized. This kind of uniquely localized deformation, however, is absent in our geometry optimization results.

## C. $I$ - $V$ characteristics

The  $I$ - $V$  characteristics of the bent structures are depicted in Fig. 5. From Fig. 5(a) it is evidently seen that as the bending angle increases, the current passing through the bent armchair (6,6) tube decreases, while that of the zigzag (10,0) tube *increases*.

In order to see the reason, we notice that the conduction of the bent tube under bias is determined by the number of conducting channels available within the two semi-infinite leads and the corresponding transmission coefficient between any pair of them, for the energies belonging to the integra-



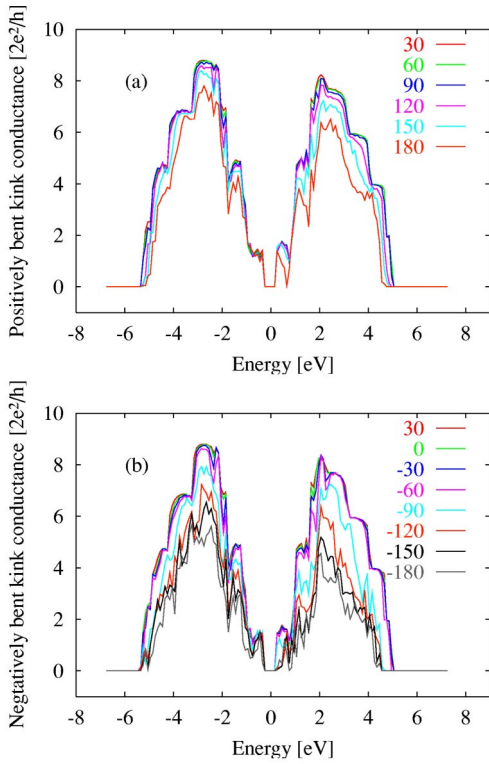


FIG. 4. (Color online) Conductance characteristics of the (10,0)-(6,6) kink structure at different positive (a) and negative (b) bending angles.

tion window  $f_B(E - \mu_B) - f_A(E - \mu_A)$  in Eq. (1). The number of conducting channels of the leads at any energy is independent of the bending angle and is determined by the number of the highest occupied bands of one lead and the number of lowest unoccupied bands of the other lead, which share the same energy after the band structures are shifted due to the applied bias. The transmission coefficient, on the other hand, depends on the deformation of the local density of states (LDOS) within the bent region, as one moves from the two ends of this region toward its center. Upon a detailed examination of the LDOS within the bent region under nonzero bias, we observe that the LDOS in the bent region includes oscillations whose amplitude increases with increasing bending angle. The increase of the amplitude, however, is not symmetric: taking the LDOS of the straight tube as reference, on the average, the “positive” amplitudes are dominant over the “negative” ones. This is attributed to the creation of additional localized electron/hole states for higher bendings.

We first consider the case of the metallic (6,6) tube, with a pseudogap of 2.0 eV. For this tube, the number of available conducting channels in one of the leads at any energy in the integration window is equal to the number of bands within the pseudogap, up to bias 2.0 V. Whenever the oscillations of the LDOS of the bent region result in a smaller number of states as compared to that of straight tube at a certain energy, the transmission coefficient is reduced—due to the reduction of the states available for tunneling across the bent region—which results in a conductance reduction. Whenever the

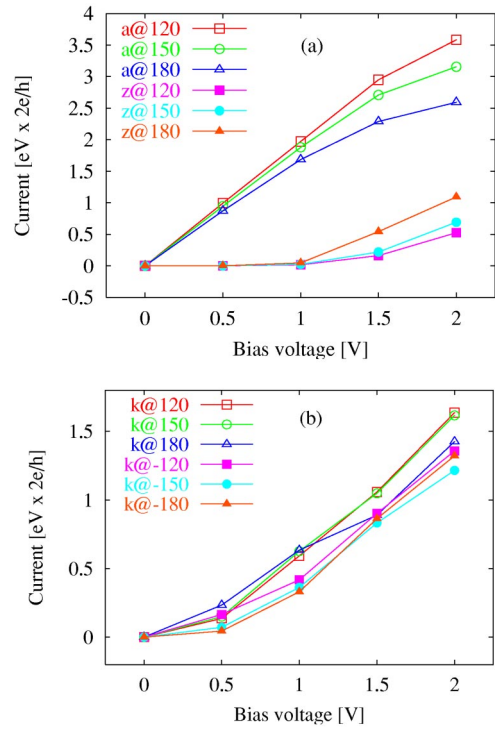


FIG. 5. (Color online) Current-voltage ( $I$ - $V$ ) characteristics of the (6,6) metallic armchair and (10,0) semiconducting zigzag (a) as well as that of (10,0)-(6,6) kink structure (b) at different bending angles.

LDOS oscillations of the bent region increase the number of states compared to that of the straight tube, however, the conductance cannot increase due to the limited number of channels within the pseudogap of one of the leads. Therefore the net effect of LDOS oscillations within the bent region is a *reduction* of the conductance and current for higher bendings. Next, consider the case of a semiconducting (10,0) tube. In this case, the number of available channels of the leads, within the integration window, is not as restricted as that of the metallic (6,6) tube. In particular, some of the van Hove singularities corresponding to the DOS of one of the leads become aligned with those of the other lead, as a result of the DOS shift due to the applied bias. Therefore, the LDOS oscillations in the bent region can result in both an increase and decrease of conductance. However, as the “positive” amplitudes in the LDOS oscillations are on the average dominant over the “negative” ones, the conductance and current *increase* at higher bending angles. This is restricted to the nonzero-bias case, as for zero-bias conductances the limiting factor is the maximum number of conducting channels of leads and the situation is similar to that of the metallic (6,6) case described above.

The  $I$ - $V$  characteristics of the kink structure at different bending angles, which are displayed in Fig. 5(b), do not show a monotonic increase or decrease of the current upon bending. This is attributed to the fact that for the (10,0)-(6,6) kink structure, the mechanisms responsible for an increase or decrease of the current in individual (6,6) and (10,0) struc-

tures compete with each other and prevent a net, bending-dependent increase or decrease of the current from being present.

The monotonic change of the current upon bending, at fixed bias voltage, is an interesting effect which can be employed in designing nanometer-scale electromechanical sensors and switches. The difference in the localization patterns of the electron/hole states within the bent region, together with the available conducting channels in the leads, results in opposite bending-dependent behaviors of the  $I$ - $V$  characteristics for the metallic and semiconducting tubes. However, each of these behaviors makes it possible to establish a correspondence between the bending angle and the current, at a fixed bias, which is passing through the bent tube. According to our results, the bending dependence of the current is more significant at higher bias voltages and shows a stronger dependence of the electronic transport characteristics on the mechanical response of the nanotubes upon bending. For example, the  $I$ - $V$  results of the semiconducting (10,0) tube show that it is possible to switch from a relatively small current ( $0.161 \times eV \times 2e/h$ ) to a relatively large one ( $0.542 \times eV \times 2e/h$ ), by just bending the tube from  $120^\circ$  to  $180^\circ$  at a fixed bias voltage of 1.5 V.

#### IV. CONCLUSIONS

In summary, we have calculated the relaxed configurations of metallic, semiconducting, and metal-semiconductor kink nanotube structures at different bending angles. A dif-

ference between the mechanical response of the zigzag and armchair nanotubes, at relatively large bendings, is observed, which is attributed to the presence of bonds parallel to the tube's axis in the zigzag case. Although at zero applied bias the conductance of all the structures is reduced rather smoothly upon bending, at a nonzero bias the behaviors differ: While the current passing through the metallic structure decreases at larger bending angles, that of the semiconducting one increases. This is explained by the difference in the localization patterns of electron/hole states within the bent region and the available channels of the leads, which show, in addition, why the kink structure does not show such a monotonic behavior. The correspondence between the mechanical response and the electronic transport of the nanotubes is shown to be applicable to nanoelectromechanical switch and sensor design.

#### ACKNOWLEDGMENTS

The authors would like to express their sincere thanks to the crew of the Center for Computational Materials Science of the Institute for Materials Research, Tohoku University, for their continuous support of the computing facilities. The cooperation of R. Note is specially acknowledged. A.A.F., H.M., and Y.K. are supported by the Special Coordination Funds of the Ministry of Education, Culture, Sports, Science and Technology of the Japanese government. B.I.Y. is supported by NASA URETI.

\*Electronic address: amir@imr.edu

<sup>1</sup>J. P. Lu, Phys. Rev. Lett. **79**, 1297 (1997).

<sup>2</sup>D. Sánchez-Portal, E. Artacho, J. M. Soler, A. Rubio, and P. Ordejón, Phys. Rev. B **59**, 12 678 (1999).

<sup>3</sup>D. Srivastava, M. Menon, and K. Cho, Phys. Rev. Lett. **83**, 2973 (1999).

<sup>4</sup>T. Ozaki, Y. Iwasa, and T. Mitani, Phys. Rev. Lett. **84**, 1712 (2000).

<sup>5</sup>J. F. Despres, E. Daguerre, and K. Lafdi, Carbon **33**, 87 (1995).

<sup>6</sup>S. Iijima, C. Barbec, A. Maiti, and J. Bernholc, J. Chem. Phys. **104**, 2089 (1996).

<sup>7</sup>O. Lourie, D. M. Cox, and H. D. Wagner, Phys. Rev. Lett. **81**, 1638 (1998).

<sup>8</sup>T. Kizuka, Phys. Rev. B **59**, 4646 (1999).

<sup>9</sup>B. I. Yakobson, C. J. Brabec, and J. Bernholc, Phys. Rev. Lett. **76**, 2511 (1996).

<sup>10</sup>C. F. Cornwell and L. T. Wille, Solid State Commun. **101**, 555 (1997).

<sup>11</sup>A. Rochefort, D. R. Salahub, and Ph. Avouris, Chem. Phys. Lett. **297**, 45 (1998).

<sup>12</sup>A. Rochefort, Ph. Avouris, F. Lesage, and D. R. Salahub, Phys. Rev. B **60**, 13 824 (1999).

<sup>13</sup>M. B. Nardelli and J. Bernholc, Phys. Rev. B **60**, R16 338 (1999).

<sup>14</sup>S. Paulson, M. R. Falvo, N. Snider, A. Helser, T. Hudson, A. Seeger, R. M. Taylor, R. Superfine, and S. Washburn, Appl. Phys. Lett. **75**, 2936 (1999).

<sup>15</sup>P. E. Lammert, P. Zhang, and V. H. Crespi, Phys. Rev. Lett. **84**, 2453 (2000).

<sup>16</sup>D. Tekleab, D. L. Carroll, G. G. Samsonidze, and B. I. Yakobson, Phys. Rev. B **64**, 035419 (2001).

<sup>17</sup>D. Bozovic, M. Bockrath, J. H. Hafner, C. M. Lieber, H. Park, and M. Tinkham, Appl. Phys. Lett. **78**, 3693 (2001).

<sup>18</sup>T. W. Tomblor, C. Zhou, L. Alexseyev, J. Kong, H. Dai, L. Liu, C. S. Jayanthi, M. Tang, and S. Y. Wu, Nature (London) **405**, 769 (2000).

<sup>19</sup>L. Liu, C. S. Jayanthi, M. Tang, S. Y. Wu, T. W. Tomblor, C. Zhou, L. Alexseyev, J. Kong, and H. Dai, Phys. Rev. Lett. **84**, 4950 (2000).

<sup>20</sup>A. Maiti, A. Svizhenko, and M. P. Anantram, Phys. Rev. Lett. **88**, 126805 (2002).

<sup>21</sup>Ph. Lambin, A. Fonseca, J. P. Vigneron, J. B. Nagy, and A. A. Lucas, Chem. Phys. Lett. **245**, 85 (1995).

<sup>22</sup>J. Han, M. P. Anantram, R. L. Jaffe, J. Kong, and H. Dai, Phys. Rev. B **57**, 14 983 (1998).

<sup>23</sup>Z. Yao, H. W. Ch. Postma, L. Balents, and C. Dekker, Nature (London) **402**, 273 (1999).

<sup>24</sup>C. H. Xu, C. Z. Wang, C. T. Chan, and K. M. Ho, J. Phys.: Condens. Matter **4**, 6047 (1992).

<sup>25</sup>A. A. Farajian and M. Mikami, J. Phys.: Condens. Matter **13**, 8049 (2001).

<sup>26</sup>X.-P. Li, R. W. Nunes, and D. Vanderbilt, Phys. Rev. B **47**, 10 891 (1993).

<sup>27</sup>K. Ohno, K. Esfarjani, and Y. Kawazoe, *Computational Materials Science from Ab Initio to Monte Carlo Methods* (Springer, Berlin, 1999).

<sup>28</sup>The relaxation results that we report here are obtained using the

- parallel density matrix tight-binding code authored by X.-P. Li, D. Vanderbilt, R. Nunes, M. Robbins, and N. Modine (unpublished), modified to include the Broyden minimization scheme.
- <sup>29</sup>P. A. Lee and D. S. Fisher, *Phys. Rev. Lett.* **47**, 882 (1981).
- <sup>30</sup>A. MacKinnon, *Z. Phys. B: Condens. Matter* **59**, 385 (1985).
- <sup>31</sup>M. C. Muñoz, V. R. Velasco, and F. Garcia-Moliner, *Prog. Surf. Sci.* **26**, 117 (1987).
- <sup>32</sup>F. Garcia-Moliner and V. R. Velasco, *Theory of Single and Multiple Interfaces* (World Scientific, Singapore, 1992).
- <sup>33</sup>S. Datta, *Electronic Transport in Mesoscopic Systems* (Cambridge University Press, Cambridge, UK, 1995).
- <sup>34</sup>L. Chico, L. X. Benedict, S. G. Louie, and M. L. Cohen, *Phys. Rev. B* **54**, 2600 (1996).
- <sup>35</sup>A. A. Farajian, K. Esfarjani, and Y. Kawazoe, *Phys. Rev. Lett.* **82**, 5084 (1999).
- <sup>36</sup>M. Büttiker, Y. Imry, R. Landauer, and S. Pinhas, *Phys. Rev. B* **31**, 6207 (1985).
- <sup>37</sup>A. A. Farajian, K. Esfarjani, and M. Mikami, *Phys. Rev. B* **65**, 165415 (2002).
- <sup>38</sup>B. I. Yakobson, *Appl. Phys. Lett.* **72**, 918 (1998).